Journal of Innovative Applied Mathematics and Computational Sciences

J. Innov. Appl. Math. Comput. Sci. **5**(1) (2025), 97–119. DOI: 10.58205/jiamcs.v5i1.1873

http://jiamcs.centre-univ-mila.dz/

Nonlinear dynamics and chaos control of a discrete Rosenzweig-MacArthur prey-predator model

Teqwa Bouguettoucha [1], Nedjla Boukhalfa [2] and Abdelouahab Mohammed Salah [2]

[1] Department of mathematics, University of Bordj Bou-Arreridj, Algeria
[2]Laboratory of Mathematics and their Interactions, Abdelhafid Boussouf University Center of Mila, Algeria

Received December 10, 2024, Accepted July 19, 2025, Published July 24, 2025

Abstract. This paper investigates the nonlinear dynamics and chaos control of a discrete Rosenzweig-MacArthur predator-prey model. We first conduct a thorough dynamical analysis, identifying the system's equilibrium points and examining their stability conditions. The study reveals the occurrence of Flip and Neimark-Sacker bifurcations, which represent critical qualitative changes in population dynamics. Specifically, Flip bifurcations lead to period-doubling phenomena, while Neimark-Sacker bifurcations indicate the emergence of quasi-periodic oscillations, both of which are crucial for understanding the onset of complex behaviors such as cycles and oscillations in ecological systems. To address the chaotic dynamics induced by these bifurcations, two control strategies are applied: the Ott-Grebogi-Yorke (OGY) method and feedback control. The results demonstrate the effectiveness of both approaches in stabilizing the system's dynamics, with the OGY method proving to be more effective in achieving faster stabilization. These findings provide valuable insights into the management and preservation of ecological systems where predator-prey interactions exhibit instability and chaos.

Keywords: Prey-predator model, Rosenzweig-MacArthur model, stability, bifurcations, chaos control.
2020 Mathematics Subject Classification: 92B05, 39A30, 39A28, 39A33. MSC2020

1 Introduction

The analysis of dynamical systems plays a fundamental role in understanding and predicting complex phenomena across a wide range of real-world applications, including ecology, biology, engineering, and economics. Stability analysis, bifurcation theory, mixed-mode oscillations, chaos control, and synchronization are key tools used to investigate the qualitative behavior of such systems and their responses to parameter variations and external influences. These concepts have been widely applied to study periodic solutions and their stability in differential systems [9], bifurcation and chaos in electrical circuit [2,9], synchronization phenomena in chaotic systems [15], and Hopf bifurcation leading to oscillatory behavior in biological

✉Corresponding author. Email: kakar.may1996@gmail.com

and economic models [1,22]. Moreover, the investigation of nonlinear dynamics and chaotic behaviors in economic games [3,5,6,20], as well as synchronization and control in electrical circuits and memristor-based systems [11,12], has provided valuable insights for both theoretical analysis and practical applications. Recent studies have emphasized the development of efficient control strategies to suppress or stabilize chaos in various systems [**?**,17], and explored the complex dynamics of piecewise linear maps and higher-order difference equations [**?**,10]. These methodologies not only enhance the understanding of underlying mechanisms governing complex systems but also contribute to the design of robust control schemes to ensure desired performance and stability in real-life scenarios.

The Rosenzweig-MacArthur model remains a cornerstone in ecological modeling, offering a robust framework to analyze predator-prey interactions and their implications on population stability and complex dynamical behaviors. Its significance stems from its ability to incorporate both biotic and abiotic factors, providing insights into species coexistence and persistence under varying environmental conditions [21,24]. Central to this model is the Holling type II functional response, capturing the nonlinear relationship between prey availability and predator consumption, thus reflecting realistic ecological saturation effects [16,18].

Beyond classical predator-prey interactions, ecological systems are well-known for exhibiting rich nonlinear behaviors, including oscillations, periodic cycles, bifurcations, and chaotic dynamics [19]. These phenomena are highly sensitive to initial conditions and parameter variations, often leading to qualitative shifts in system behavior through bifurcations such as Flip and Neimark-Sacker types [7,25]. Understanding these bifurcations is crucial for predicting ecological stability and designing effective management and conservation strategies.

Recent research emphasizes the utility of discrete-time formulations of ecological models, such as the Rosenzweig-MacArthur model, to capture time-delayed interactions, seasonal effects, and inherent discretization in data collection [3,14]. The discrete approach facilitates the exploration of dynamical behaviors that may remain hidden in continuous models, enabling rigorous analysis of complex bifurcation structures and chaotic regimes.

Motivated by these advancements, this study investigates the bifurcation phenomena and chaotic dynamics in the discrete Rosenzweig-MacArthur model and explores effective strategies for chaos control. Specifically, we apply two well-established methods: the OGY method, which utilizes small parameter perturbations to stabilize unstable periodic orbits embedded within chaotic attractors [3,7], and feedback control, which introduces corrective forces to maintain system stability [4].

The remainder of this paper is structured as follows: Section 2 presents the mathematical formulation of the discrete Rosenzweig-MacArthur model. Section 3 provides the dynamical analysis, focusing on equilibrium points and their stability conditions. Section 4 investigates bifurcation phenomena using both theoretical and numerical approaches. Section 5 discusses the application and comparative effectiveness of chaos control techniques, including the OGY and feedback methods. Finally, Section 6 concludes with key findings and implications for ecological management and future research directions.

2 Model formulation

The Rosenzweig-MacArthur prey-predator model is a well-established framework for studying population dynamics. This section formulates the model in both continuous and discrete time, emphasizing the mathematical derivation of its discrete-time version.

2.1 Continuous-time model

The continuous-time Rosenzweig-MacArthur model is defined by the following system of differential equations [16,18,24]:

$$\begin{aligned} \frac{dx}{dt} &= rx\left(1-\frac{x}{K}\right) - h(x)y, \\ \frac{dy}{dt} &= -my + ch(x)y, \end{aligned} \tag{2.1}$$

where:

- $x(t)$: Prey population at time t,
- $y(t)$: Predator population at time t,
- r: Intrinsic growth rate of prey,
- K: Carrying capacity of the prey population,
- m: Mortality rate of the predator,
- c: Conversion efficiency of prey biomass into predator biomass,
- $h(x)$: Functional response rate of predators to prey, given by the Holling Type II response [21]:

  $$h(x) = \frac{bx}{1+b\tau x}, \tag{2.2}$$

  where b is the predation rate coefficient and τ is the handling time of prey.

The term $rx\left(1-\frac{x}{K}\right)$ represents logistic growth of prey, while $h(x)y$ accounts for predation. The term $-my$ captures predator mortality, and $ch(x)y$ represents predator reproduction proportional to prey consumption.

2.2 Discrete-time model

To study population dynamics over successive generations or time steps, we derive a discrete-time version of the model using the forward Euler method [7]. The Euler approximation of (2.1) with a time step $\Delta t = h$ is given by:

$$\begin{aligned} x_{t+1} &= x_t + h\left[rx_t\left(1-\frac{x_t}{K}\right) - \frac{bx_ty_t}{x_t+H}\right], \\ y_{t+1} &= y_t + h\left[y_t\left(-m+\frac{cx_t}{x_t+H}\right)\right]. \end{aligned} \tag{2.3}$$

Here, $H = \frac{1}{s\tau}$ is the Half-saturation constant of the functional response,

The discrete formulation captures nonlinear and time-delayed interactions, facilitating the analysis of complex behaviors like bifurcations and chaos [7,16].

3 Dynamical analysis

This section provides a rigorous examination of the discrete Rosenzweig-MacArthur prey-predator model, focusing on equilibrium points, their stability, and bifurcations. The results are presented as lemmas, propositions, and theorems, accompanied by detailed proofs.

3.1 Equilibrium points and stability analysis

Lemma 3.1 (Equilibrium Points)**.** *The system admits the following equilibrium points:*

For all b, c, m, r, H, h, K the discrete system (2.3) admits a trivial equilibrium $P_1 = (0, 0)$, representing extinction of both prey and predator populations, and a semi-trivial equilibrium $P_2 = (K, 0)$, where the prey population exists at carrying capacity K, while the predator population is extinct.

A coexistence equilibrium $P_3 = (x^*, y^*)$, for $c > \max\{m, \frac{mH+K}{K}\}$ where:

$$x^* = \frac{Hm}{c-m}, \quad y^* = \frac{cHr(K(c-m) - Hm)}{bK(c-m)^2}.$$

Proof. To find equilibrium points, solve $x_{t+1} = x_t$ and $y_{t+1} = y_t$:

$$x = x\left(1 + hr - \frac{hr}{K}x - \frac{hbxy}{x+H}\right), \quad y = y\left(1 - hm + \frac{chx}{x+H}\right).$$

From the first equation, $x = 0$ or:

$$hr - \frac{hr}{K}x - \frac{hby}{x+H} = 0.$$

Similarly, from the second equation, $y = 0$ or:

$$-hm + \frac{chx}{x+H} = 0.$$

By substituting $y = 0$ in the first equation, we find $x = K$, giving the semi-trivial equilibrium $P_2 = (K, 0)$. For the coexistence equilibrium P_3, solve the equations:

$$hr - \frac{hr}{K}x - \frac{hby}{x+H} = 0, \quad -hm + \frac{chx}{x+H} = 0,$$

which yield:

$$x^* = \frac{Hm}{c-m}, \quad y^* = \frac{cHr(K(c-m) - Hm)}{bK(c-m)^2}.$$

The condition $c > \max\{m, \frac{mH+K}{K}\}$ ensures positivity of x^* and y^*. □

Proposition 3.2 (Stability of the fixed point P_1)**.** *For the discrete-time model (2.3), the stability characteristics of the fixed point $P_1 = (0, 0)$ are as follows:*

(i) P_1 can never be a sink.

(ii) P_1 will be a source when $m > \frac{2}{h}$.

(iii) P_1 is a saddle for $0 < m < \frac{2}{h}$.

(iv) P_1 becomes non-hyperbolic when $m = \frac{2}{h}$.

Proof. The stability of a fixed point is determined by the eigenvalues of the Jacobian matrix evaluated at that point. For the discrete-time model (2.3), the Jacobian matrix is expressed at P_1 as:

$$J|_{P_1} = \begin{pmatrix} 1 + hr & 0 \\ 0 & 1 - hm \end{pmatrix}.$$

The eigenvalues are:

$$\lambda_1 = 1 + hr, \quad \lambda_2 = 1 - hm.$$

Since $r > 0$ in the context of this model, λ_1 is always greater than 1, and P_1 cannot behave as a sink.

$$|\lambda_2| < 1 \text{ implies } -1 < 1 - hm < 1 \text{ then } 0 < m < \frac{2}{h}.$$

Interpretation:

- If $m > \frac{2}{h}$, $\lambda_2 > 1$, causing P_1 to act as a source.
- If $0 < m < \frac{2}{h}$, $\lambda_1 > 1$ and $\lambda_2 < 1$, making P_1 a saddle.
- If $m = \frac{2}{h}$, $\lambda_2 = -1$, resulting in P_1 being non-hyperbolic.

□

Proposition 3.3 (Stability of the fixed point P_2)**.** *For the discrete-time model* (2.3)*, the stability characteristics of the fixed point $P_2 = (K, 0)$ are as follows:*

(i) P_2 is a sink if $\frac{-2H+hmH}{2-hm+ch} < K < \frac{hmH}{cH-hm}$ and $0 < r < \frac{2}{h}$.

(ii) P_2 is a source if $K < \frac{-2H+hmH}{2-hm+ch}$ and $r > \frac{2}{h}$.

(iii) P_2 is a saddle if $K < \frac{-2H+hmH}{2-hm+ch}$ and $0 < r < \frac{2}{h}$.

(iv) P_2 is non-hyperbolic if $K = \frac{-2H+hmH}{2-hm+ch}$ or $r = \frac{2}{h}$.

Proof. At $P_2 = (K, 0)$, the Jacobian matrix becomes:

$$J|_{P_2} = \begin{pmatrix} 1 - hr & \dfrac{-bhK}{K+h} \\ 0 & 1 - hm + \frac{chK}{H+K} \end{pmatrix}.$$

The eigenvalues are:

$$\lambda_1 = 1 - hr, \quad \lambda_2 = 1 - hm + \frac{chK}{H+K}.$$

Stability Conditions:

$$|\lambda_1| < 1 \text{ implies that } -1 < 1 - hr < 1 \text{ then, } r < \frac{2}{h}.$$

$$|\lambda_2| < 1 \text{ implies that } -1 < 1 - hm + \frac{chK}{H+K} < 1.$$

Splitting the inequality:

$$1 - hm + \frac{chK}{H+K} > -1 \text{ implies that } \frac{chK}{H+K} > -2 + hm,$$

and:

$$1 - hm + \frac{chK}{H+K} < 1 \text{ implies that } \frac{chK}{H+K} < 2 - hm.$$

Combining these conditions:

$$\frac{-2H + hmH}{2 - hm + ch} < K < \frac{hmH}{cH - hm}.$$

Interpretation:

- If $\frac{-2H+hmH}{2-hm+ch} < K < \frac{hmH}{cH-hm}$ and $r < \frac{2}{h}$, P_2 is a sink.
- If $K < \frac{-2H+hmH}{2-hm+ch}$ and $r > \frac{2}{h}$, P_2 acts as a source.
- If $K < \frac{-2H+hmH}{2-hm+ch}$ and $r < \frac{2}{h}$, P_2 is a saddle.
- If $K = \frac{-2H+hmH}{2-hm+ch}$ or $r = \frac{2}{h}$, P_2 is non-hyperbolic.

□

Proposition 3.4 (Stability of the fixed point P_3)**.** *For the fixed point P_3 of model (2.3), the stability depends on the sign of the discriminant Δ of the Jacobian's characteristic equation and the parameter K. The results are as follows:*

- ***Case 1:*** $\Delta < 0$
  - *(i)* *P_3 is a stable focus if* $0 < K < \frac{H(hcm+c+m-hm^2)}{(c-m)(1+ch-hm)}$*, provided* $c > \max\left\{m, \frac{hm-1}{h}, \frac{hm^2-m}{hm+1}\right\}$.
  - *(ii)* *P_3 is an unstable focus if* $K > \frac{H(hcm+c+m-hm^2)}{(c-m)(1+ch-hm)}$.
  - *(iii)* *P_3 is non-hyperbolic if* $K = \frac{H(hcm+c+m-hm^2)}{(c-m)(1+ch-hm)}$.
- ***Case 2:*** $\Delta > 0$
  - *(i)* *P_3 is a stable node if:*

$$\frac{mH}{c-m} < K < \frac{hHmr(-2c-2m-hmc+hm^2)}{(h^2m^2r-4c-h^2mrc-2hmr)(c-m)},$$

  with $c < \min\left\{\frac{h^2m^2r-2hmr}{4+h^2mr}, \frac{hm^2-2m}{mh+2}\right\}$ *and* $c > m$.
  - *(ii)* *P_3 is an unstable node if:*

$$\frac{hHmr(-2c-2m-hmc+hm^2)}{(h^2m^2r-4c-h^2mrc-2hmr)(c-m)} < K < \frac{mH}{c-m}.$$

  - *(iii)* *P_3 is non-hyperbolic if:*

$$K = \frac{mH}{c-m} \quad \text{or} \quad K = \frac{hHmr(-2c-2m-hmc+hm^2)}{(h^2m^2r-4c-h^2mrc-2hmr)(c-m)}.$$

Proof. The stability of the fixed point P_3 is determined by the eigenvalues of the Jacobian matrix. The eigenvalues are roots of the characteristic equation:

$$\lambda^2 - \mathrm{Tr}(J)\lambda + \det(J) = 0,$$

where the trace and determinant of the Jacobian are given by:

$$\mathrm{Tr}(J) = 2 - hmr\frac{c(H-K)+m(H+K)}{cK(c-m)},$$

$$\det(J) = 1 - hmr\frac{c(H-K)+m(H+K)}{cK(c-m)} + h^2mr\frac{cK-m(H+K)}{cK}.$$

The discriminant of the characteristic equation is:

$$\Delta = \mathrm{Tr}(J)^2 - 4\det(J).$$

—

When $\Delta < 0$, the eigenvalues are complex conjugates, and the fixed point behaves as a focus. The stability depends on the real part of the eigenvalues, given by $\frac{\mathrm{Tr}(J)}{2}$. Substituting the expression for $\mathrm{Tr}(J)$, the fixed point is:

- A **stable focus** if $\mathrm{Tr}(J) < 0$, which occurs when $0 < K < \frac{H(hcm+c+m-hm^2)}{(c-m)(1+ch-hm)}$, provided $c > \max\left\{m, \frac{hm-1}{h}, \frac{hm^2-m}{hm+1}\right\}$.
- An **unstable focus** if $\mathrm{Tr}(J) > 0$, which occurs when $K > \frac{H(hcm+c+m-hm^2)}{(c-m)(1+ch-hm)}$.
- **Non-hyperbolic** if $\mathrm{Tr}(J) = 0$, which occurs when $K = \frac{H(hcm+c+m-hm^2)}{(c-m)(1+ch-hm)}$.

—

When $\Delta > 0$, the eigenvalues are real and distinct, and the fixed point behaves as a node. The stability depends on the signs of the eigenvalues:

- A **stable node** if both eigenvalues are negative, which occurs when:

$$\frac{mH}{c-m} < K < \frac{hHmr(-2c-2m-hmc+hm^2)}{(h^2m^2r-4c-h^2mrc-2hmr)(c-m)},$$

  with $c < \min\left\{\frac{h^2m^2r-2hmr}{4+h^2mr}, \frac{hm^2-2m}{mh+2}\right\}$ and $c > m$.

- An **unstable node** if at least one eigenvalue is positive, which occurs when:

$$\frac{hHmr(-2c-2m-hmc+hm^2)}{(h^2m^2r-4c-h^2mrc-2hmr)(c-m)} < K < \frac{mH}{c-m}.$$

- **Non-hyperbolic** if one eigenvalue is zero, which occurs when:

$$K = \frac{mH}{c-m} \quad \text{or} \quad K = \frac{hHmr(-2c-2m-hmc+hm^2)}{(h^2m^2r-4c-h^2mrc-2hmr)(c-m)}.$$

□

3.2 Bifurcation analysis

Bifurcations represent parameter values at which the system's qualitative dynamics change, leading to complex behaviors like periodicity or chaos.

Thus, bifurcation analysis is crucial for understanding how environmental factors and inter-species interactions drive ecosystem stability or instability.

Bifurcation at P_1:

When the non-hyperbolic condition $m = \frac{2}{h}$ is fulfilled the Jacobian matrix at P_1 has $\lambda_2|_{m=\frac{2}{h}} = -1$ but $\lambda_1|_{m=\frac{2}{h}} = 1 + hr \neq \pm 1$. This implies that at P_1 the under study model (2.3) may undergoes a flip bifurcation when (b, c, m, r, H, h, K) passes through the region:

$$F|_{P_1} = \left\{ (b, c, K, m, r, H, h) \in \mathbb{R}_+^{*7} / m = \frac{2}{h} \right\}.$$

Theorem 3.5. *The model (2.3) undergoes a flip bifurcation at P_1 when (b, c, m, r, H, h, K) passes through the region:*

$$F|_{P_1} = \left\{ (b, c, K, m, r, H, h) \in \mathbb{R}_+^{*7} / m = \frac{2}{h} \right\}.$$

Proof. To analyze the bifurcation at P_1 when $m = \frac{2}{h}$ we use the predator update function:

$$g(x, y, m) = y + hy \left(-m + \frac{cx}{x + H} \right).$$

We check the flip conditions at the first fixed point P_1, when $m = \frac{2}{h}$:

- $\frac{\partial g}{\partial y}(x, y, m) = 1 + h(-m + \frac{cx}{x+H})$. Thus, $\frac{\partial g}{\partial y}(x, y, m) \mid_{(P_1, \frac{2}{h})} = -1$.
- $\alpha = \frac{\partial^2 g}{\partial m \partial y}(x, y, m) + \frac{1}{2} \frac{\partial g}{\partial m}(x, y, m) \frac{\partial^2 g}{\partial y^2}(x, y, m) \mid_{(P_1, \frac{2}{h})} = -h \neq 0.$
- $\beta = \frac{1}{3!} \frac{\partial^3 g}{\partial y^3}(x, y, m) + \frac{1}{2!} \left(\frac{\partial g}{\partial y}(x, y, m) \right)^2 \mid_{(P_1, \frac{2}{h})} = \frac{1}{2} \neq 0.$

So we have a flip bifurcation through P_1 if $(b, c, K, m, r, H, h) \in F|_{P_1}$. □

Bifurcation at P_2

The bifurcation analysis at the fixed point P_2 focuses on the conditions under which the system undergoes a flip bifurcation. The eigenvalues of the Jacobian matrix at P_2 determine the presence or absence of this bifurcation.

Case 1: $r = \frac{2}{h}$ and $hm \neq \frac{chK}{H+K}$ When $r = \frac{2}{h}$ and $hm \neq \frac{chK}{H+K}$, we have:

$$\lambda_1|_{r=\frac{2}{h}} = -1, \quad \lambda_2|_{r=\frac{2}{h}} = 1 - hm + \frac{chK}{H + K} \neq \pm 1.$$

This implies that if the parameter set (b, c, K, m, r, H, h) lies on the region:

$$F_1|_{P_2} = \left\{ (b, c, K, m, r, H, h) \in \mathbb{R}_+^{*7} \middle| r = \frac{2}{h}, hm \neq \frac{chK}{H + K} \right\},$$

the model (2.3) may undergo a flip bifurcation at P_2.

Theorem 3.6 ([8]). *If $(b, c, K, m, r, H, h) \in F_1|_{P_2}$, then a flip bifurcation occurs at P_2.*

Proof. To verify the flip bifurcation conditions at P_2 when $r = \frac{2}{h}$, we use the prey update function:

$$f(x, y, r) = x + hrx - \frac{hrx^2}{K} - \frac{hbxy}{x + H}.$$

we have

$$\frac{\partial f}{\partial x}(x,y,r) = 1 + hr - 2\frac{hr}{K}x - \frac{hbHy}{(x+H)^2}.$$

At $(P_2, r = \frac{2}{h})$, we find:

$$\frac{\partial f}{\partial x}|_{(P_2, r=\frac{2}{h})} = -1.$$

On the other hand we have

$$\alpha = \frac{\partial^2 f}{\partial r \partial x} + \frac{1}{2}\frac{\partial f}{\partial r}\frac{\partial^2 f}{\partial x^2}|_{(P_2, r=\frac{2}{h})}.$$

Then

$$\alpha = -h \neq 0.$$

Finally we have

$$\beta = \frac{1}{3!}\frac{\partial^3 f}{\partial x^3} + \frac{1}{2}\left(\frac{\partial f}{\partial x}\right)^2 |_{(P_2, r=\frac{2}{h})}.$$

At $(P_2, r = \frac{2}{h})$:

$$\beta = \frac{1}{2} \neq 0.$$

Since $\alpha \neq 0$ and $\beta \neq 0$, the non-degeneracy conditions for a flip bifurcation are satisfied. Therefore, a flip bifurcation occurs at P_2 when $(b, c, K, m, r, H, h) \in F_1|_{P_2}$. □

Case 2: $K = \frac{-2H+hmH}{2-hm+ch}$ When $K = \frac{-2H+hmH}{2-hm+ch}$, the eigenvalues are:

$$\lambda_1|_{K=\frac{-2H+hmH}{2-hm+ch}} = 1 - hr \neq \pm 1, \quad \lambda_2|_{K=\frac{-2H+hmH}{2-hm+ch}} = -1.$$

This implies that if the parameter set (b, c, m, r, H, h, K) lies on the region

$$F_2|_{P_2} = \left\{(b, c, K, m, r, H, h) \in \mathbb{R}_+^{*\,7} | K = \frac{-2H + hmH}{2 - hm + ch}\right\},$$

the model (2.3) may undergo a flip bifurcation at P_2.

Theorem 3.7 ([8]). *If $(b, c, K, m, r, H, h) \in F_2|_{P_2}$, flip bifurcation occurs at P_2.*

Proof. To verify the bifurcation conditions at P_2 when $K = \frac{-2H+hmH}{2-hm+ch}$, we calculate the derivatives of the prey update function:

$$f(x,y,K) = x + hrx - \frac{hrx^2}{K} - \frac{hbxy}{x+H}.$$

The first derivative of $f(x,y,K)$ with respect to x is:

$$\frac{\partial f}{\partial x}(x,y,K) = 1 + hr - 2\frac{hr}{K}x - \frac{hbHy}{(x+H)^2}.$$

At $P_2 = (K, 0)$, substituting $y = 0$, we find:

$$\frac{\partial f}{\partial x}|_{K=\frac{-2H+hmH}{2-hm+ch}} = 1 + hr - 2\frac{hr}{K}K = -1.$$

The second derivative with respect to x is:

$$\frac{\partial^2 f}{\partial x^2}(x,y,K) = -2\frac{hr}{K} + \frac{2hbHy}{(x+H)^3}.$$

At $P_2 = (K,0)$, where $y = 0$, this simplifies to:

$$\frac{\partial^2 f}{\partial x^2}\Big|_{K=\frac{-2H+hmH}{2-hm+ch}} = -2\frac{hr}{K}.$$

The mixed second derivative with respect to K and x is:

$$\frac{\partial^2 f}{\partial K \partial x}(x,y,K) = \frac{hrx^2}{K^2}.$$

At $P_2 = (K,0)$, substituting $x = K$, this becomes:

$$\frac{\partial^2 f}{\partial K \partial x}\Big|_{K=\frac{-2H+hmH}{2-hm+ch}} = \frac{hr}{K}.$$

The coefficient α is:

$$\alpha = \frac{\partial^2 f}{\partial K \partial x} + \frac{1}{2}\frac{\partial^2 f}{\partial x^2}\frac{\partial f}{\partial K}.$$

The partial derivative with respect to K is:

$$\frac{\partial f}{\partial K} = \frac{hrx^2}{K^2}.$$

At $P_2 = (K,0)$, substituting $x = K$, this becomes:

$$\frac{\partial f}{\partial K}\Big|_{K=\frac{-2H+hmH}{2-hm+ch}} = \frac{hr}{K}.$$

Substituting, we find:

$$\alpha = \frac{hr}{K} + \frac{1}{2}\left(-2\frac{hr}{K}\right)\left(\frac{hr}{K}\right) = \frac{hr}{K} - \frac{hr^2}{K} = \frac{hr(1-r)}{K}.$$

Since $hr > 0$, $\alpha \neq 0$.

The third derivative with respect to x is:

$$\frac{\partial^3 f}{\partial x^3}(x,y,K) = \frac{6hbHy}{(x+H)^4}.$$

At $P_2 = (K,0)$, where $y = 0$, this reduces to:

$$\frac{\partial^3 f}{\partial x^3}\Big|_{K=\frac{-2H+hmH}{2-hm+ch}} = 0.$$

The coefficient β is:

$$\beta = \frac{1}{3!}\frac{\partial^3 f}{\partial x^3} + \frac{1}{2}\left(\frac{\partial f}{\partial x}\right)^2.$$

Substituting $\frac{\partial^3 f}{\partial x^3} = 0$ and $\frac{\partial f}{\partial x} = -1$:

$$\beta = \frac{1}{3!}(0) + \frac{1}{2}(-1)^2 = \frac{1}{2} \neq 0.$$

Since $\frac{\partial f}{\partial x}\big|_{K=\frac{-2H+hmH}{2-hm+ch}} = -1$, $\alpha \neq 0$ and $\beta \neq 0$, the bifurcation conditions for a flip bifurcation are satisfied at $K = \frac{-2H+hmH}{2-hm+ch}$. □

Bifurcation at P_3

- When the bifurcation parameter K satisfies:

$$K = \frac{H(hcm + c + m - hm^2)}{(c - m)(1 + ch - hm)},$$

the fixed point P_3 becomes non-hyperbolic, as the eigenvalues of the Jacobian matrix satisfy:

$$|\lambda_{1,2}|_{K=\frac{H(hcm+c+m-hm^2)}{(c-m)(1+ch-hm)}} = 1.$$

This suggests that the system may undergo a Neimark-Sacker bifurcation through P_3.

Theorem 3.8 (Neimark-Sacker bifurcation through P_3)**.**
The discrete model (2.3) *undergoes a Neimark-Sacker bifurcation through the fixed point P_3, with K as the bifurcation parameter at the critical region*

$$N|_{P_3} = \left\{(b, c, m, r, H, h, K) \in \mathbb{R}^7_+ / K = \frac{H(hcm + c + m - hm^2)}{(c - m)(1 + ch - hm)}\right\},$$

then

Proof. To analyze the Neimark-Sacker bifurcation through P_3, let $K = K^* + \epsilon$, where $\epsilon \ll 1$ is a small perturbation around the critical bifurcation value K^*. Substituting K into the discrete model:

$$x_{t+1} = x_t + hrx_t - \frac{hrx_t^2}{K^* + \epsilon} - \frac{hbx_t y_t}{x_t + H},$$
$$y_{t+1} = y_t + hy_t \left(-m + \frac{cx_t}{x_t + H}\right).$$

The Jacobian matrix at the fixed point P_3 is given by:

$$J|_{P_3} = \begin{bmatrix} 1 + hr - \frac{2hrx^*}{K^*+\epsilon} - \frac{hbHy^*}{(x^*+H)^2} & -\frac{hbx^*}{x^*+H} \\ \frac{hcHy^*}{(x^*+H)^2} & 1 - hm + \frac{chx^*}{x^*+H} \end{bmatrix}.$$

The eigenvalues $\lambda_{1,2}$ of $J|_{P_3}$ satisfy the characteristic equation:

$$\lambda^2 - T\lambda + D = 0, \quad T = \text{tr}(J|_{P_3}), \quad D = \det(J|_{P_3}).$$

Expanding T and D in terms of ϵ, we have:

$$T(\epsilon) = T_0 + T_1\epsilon + \mathcal{O}(\epsilon^2), \quad D(\epsilon) = D_0 + D_1\epsilon + \mathcal{O}(\epsilon^2),$$

where T_0 and D_0 are evaluated at $K = K^*$.

The eigenvalues $\lambda_{1,2}$ are expressed as:

$$\lambda_{1,2}(\epsilon) = \frac{T(\epsilon) \pm i\sqrt{4D(\epsilon) - T(\epsilon)^2}}{2}.$$

Step 1: Non-Hyperbolic Condition At the bifurcation value $K = K^*$, the eigenvalues satisfy:

$$|\lambda_{1,2}| = 1.$$

This implies that P_3 is non-hyperbolic. For this to occur, the trace T and determinant D must satisfy:

$$T^2 - 4D = 0.$$

Step 2: Derivative of the Eigenvalue Modulus To confirm the Neimark-Sacker bifurcation, we calculate the derivative of the eigenvalue modulus $|\lambda|$ with respect to K. Using the characteristic equation, the eigenvalues are:

$$\lambda_{1,2} = \frac{T \pm i\sqrt{4D - T^2}}{2}.$$

The modulus of the eigenvalues is:

$$|\lambda| = \sqrt{D}.$$

Differentiating with respect to K:

$$\frac{d|\lambda|}{dK} = \frac{1}{2|\lambda|}\frac{dD}{dK}.$$

From the explicit expressions for T and D, the derivative $\frac{dD}{dK}$ is:

$$\frac{dD}{dK} = \frac{hmr(c-m)(1+ch-hm)^2}{2cH(c+m+chm-hm^2)}.$$

Step 3: Transversality Condition The transversality condition for a Neimark-Sacker bifurcation requires:

$$\frac{d|\lambda|}{dK} \neq 0.$$

Substituting the derivative of D, we confirm that:

$$\frac{hmr(c-m)(1+ch-hm)^2}{2cH(c+m+chm-hm^2)} \neq 0,$$

for all $(b, c, m, r, H, h, K) \in N|_{P_3}$.

For a Neimark-Sacker bifurcation to occur, the following conditions must hold: 1. The modulus of the eigenvalues is equal to 1 at $K = K^*$:

$$|\lambda_{1,2}(0)| = \sqrt{D_0} = 1.$$

2. The real part of $d|\lambda|/d\epsilon$ at $\epsilon = 0$ is non-zero:

$$\left.\frac{d|\lambda|}{d\epsilon}\right|_{\epsilon=0} = \frac{hmr(c-m)(1+ch-hm)^2}{2cH(c+m+chm-hm^2)} \neq 0.$$

Since both conditions are satisfied under the given parameter set $(b, c, m, r, H, h, K) \in N|_{P_3}$, the fixed point P_3 undergoes a Neimark-Sacker bifurcation. □

- If $K = \frac{mH}{c-m}$ (non-hyperbolic condition), we have: $\lambda_1 |_{K=\frac{mH}{c-m}} = 1$ but $\lambda_2 |_{K=\frac{mH}{c-m}} = 1 - hr \neq \pm 1$. This implies that if (b, c, m, r, H, h, K) passes through the following curve then at P_3 there may exists fold bifurcation:

$$F_3 |_{P_3} = \left\{ (b, c, m, r, H, h, K) \in \mathbb{R}_+^{*\,7} / K = \frac{mH}{c-m} \right\}.$$

Theorem 3.9.
If $(b, c, K, m, r, H, h) \in F_{|_{P_3}}$, then the discrete model described in (2.3) cannot undergo a fold bifurcation at P_3.

- If $K = \frac{hHmr(-2c-2m-hmc+hm^2)}{(h^2m^2r-4c-h^2mrc-2hmr)(c-m)}$ $\lambda_1 \mid_{K=\frac{hHmr(-2c-2m-hmc+hm^2)}{(h^2m^2r-4c-h^2mrc-2hmr)(c-m)}} = -1$,

$\lambda_2 \mid_{K=\frac{hHmr(-2c-2m-hmc+hm^2)}{(h^2m^2r-4c-h^2mrc-2hmr)(c-m)}} = \frac{c(-2+hm(-3+hr))-m(2+hm(-3+hr))}{m(-2+hm)-c(2+hm)} \neq \pm 1$ This implies that if (b, c, m, r, H, h, K) passes through the following curve then system(2.3) may undergoes a Flip bifurcation at P_3:

$$F_4 \mid_{P_3} = \left\{ (b, c, m, r, H, h, K) \in \mathbb{R}_+^{*\,7} / K = \frac{hHmr(-2c-2m-hmc+hm^2)}{(h^2m^2r-4c-h^2mrc-2hmr)(c-m)} \right\}.$$

Theorem 3.10. *[8]*
If $(b, c, m, r, H, h, K) \in F_4 \mid_{P_3}$, then the discrete model described in (2.3) undergoes a flip bifurcation at P_3.

Example 3.11.
Consider the set of parameter values:

$$b = 0.9, c = 3.5, H = 0.7, m = 0.7, r = 2.8, h = 1 \tag{3.1}$$

With $K \in [0.1, 0.55]$ as a bifurcation parameter and starting from the initial conditions $(x_0, y_0) = (0.1760, 0.5259)$. The Lyapunov exponent and the bifurcation diagrams are drawn versus K in figure (3.1a). The discrete model (2.3) has an equilibrium solution $P_3 = (0.1750, 0.5249)$ and the Jacobian matrix is :

$$J^c \mid_{P_3} = \begin{pmatrix} -1.1522 & -0.1800 \\ 1.6795 & 1 \end{pmatrix}.$$

With the eigenvalues $\lambda_1 = -1$ and $\lambda_2 = 0.8489 \neq \pm 1$ and hence based on these simulations one can obtain that $(b, c, H, m, r, h, K) = (0.9, 3.5, 0.7, 0.7, 2.8, 1, 0.2168) \in F_3 \mid_{P_3}$.

$$\begin{cases} \beta_{11} &= -1.1522, \\ \beta_{12} &= -0.1800, \\ \beta_{13} &= -12.4215, \\ \beta_{14} &= -0.8229, \\ \delta_{01} &= 20.8501, \\ \delta_{02} &= 59.5716, \\ \beta_{21} &= 1.6795, \\ \beta_{22} &= 1, \\ \beta_{23} &= -1.9195, \\ \beta_{24} &= 3.2. \end{cases} \tag{3.2}$$

$$\begin{cases} C_0 &= C_3 = 0, \\ C_1 &= 0.8055, \\ C_2 &= -11.2991. \end{cases} \tag{3.3}$$

And:

$$\begin{cases} h_1 &= -15.3803, \\ h_2 &= 23.8379, \\ h_3 &= -163.5835, \\ h_4 &= -269.3474, \\ h_5 &= -144.6623. \end{cases} \tag{3.4}$$

Substituting (3.4) one gets: $\Gamma_1 = 23.8379 \neq 0$, $\Gamma_2 = 91.8928 > 0$. Since $\Gamma_2 = 91.8928 > 0$ and so it can be concluded that stable period-2 points bifurcate from $P_3 = (0.175, 0.5249)$.

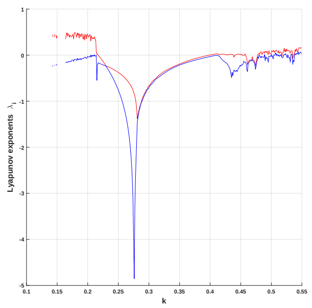

(a) Evolution of the Lyapunov exponents with respect to K, illustrating transitions between regular and chaotic dynamics.

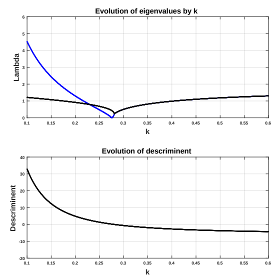

(b) Variation of eigenvalues (λ_1, λ_2) and discriminant Δ of the Jacobian matrix at the fixed point $P_3 = (0.175, 0.5249)$ with respect to K, indicating stability changes and potential bifurcations.

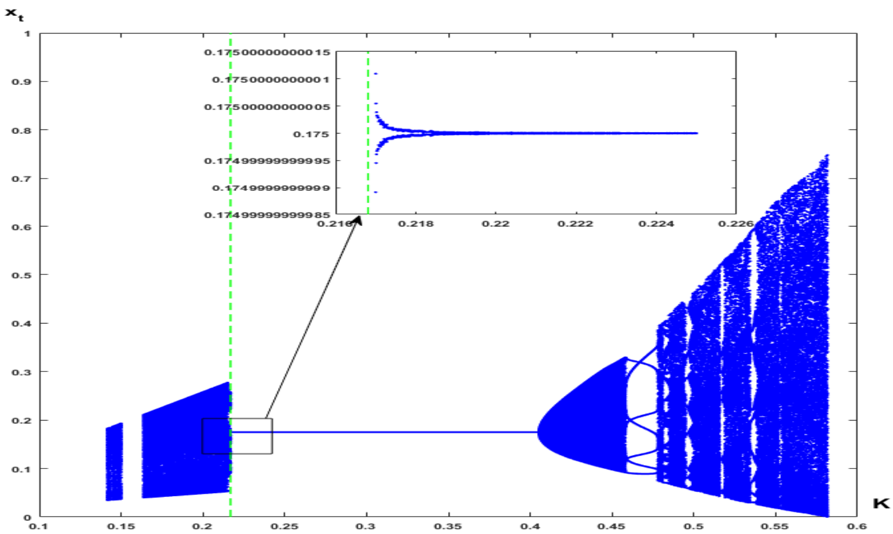

(c) Bifurcation diagram for the prey population x_t, demonstrating the system's long-term behavior and highlighting different transition scenarios leading to chaos.

Figure 3.1: Dynamical behavior of the discrete Rosenzweig-MacArthur model (2.3) at the fixed point $P_3 = (0.175, 0.5249)$ as a function of the carrying capacity $K \in [0.1, 0.55]$, using the parameter set (3.1).

3.3 Coexistence of attractors

In this section, we explain the chaotic coexistence in the Rosenzweig-MacArthur system. Table 3.1 illustrates the cases of changes in attractors and Lyapunov exponents with the evolution of K.

In the diagram, we observe the coexistence of different attractors for several values of k, such as k=0.2171 and k=0.47, with different initial conditions.

Attractors	K	$\lambda_{1,2}$
Chaotic	[0.164, 0.2169]	$\lambda_1 > 0$ and $\lambda_2 < 0$
Quasi-periodic	0.217	$\lambda_1 = 0$ and $\lambda_2 < 0$
Periodic	[0.217, 0.399]	$\lambda_1 < 0$ and $\lambda_2 < 0$
chaotic	[0.3992, 0.437]	$\lambda_1 > 0$ and $\lambda_2 < 0$
Quasi-periodic	0.438	$\lambda_1 = 0$ and $\lambda_2 < 0$
periodic	[0.438, 0.442]	$\lambda_1 < 0$ and $\lambda_2 < 0$
Quasi-periodic	0.457	$\lambda_1 = 0$ and $\lambda_2 < 0$
Periodic	[0.457, 0.477]	$\lambda_1 < 0$ and $\lambda_2 < 0$
Chaotic	[0.477, 0.538]	$\lambda_1 > 0$ and $\lambda_2 < 0$
Hyper-chaotic	[0.538, 0.5816]	$\lambda_1 > 0$ and $\lambda_2 > 0$

Table 3.1: The Lyapunov exponents and the type of attractors of the system with the first set of parameters (3.1) at $P_3 = (0.175, 0.5249)$

- If k=0.2171 with three initial conditions for $(x_1, y_1) = (0.1749, 0.5278)$ we have a chaotic attractor, for $(x_2, y_2) = (0.2505, 0.1405)$ we have(periodic points), for $(x_3, y_3) = (0.1931, 0)$ (invariant curve), where we observe two periodic points, corresponding to two Lyapunov exponent values, both of which are negative (periodic attractor), (see figure 3.3*a*,3.3*b*)
- If k=0.47 with three initial conditions for $(x_1, y_1) = (0.1831, 0.9633)$ we have a periodic points , for $(x_2, y_2) = (0.1750, 1.4346)$ we have (periodic points), for $(x_3, y_3) = (0.5886, 0)$ (invariant curve), where observe seven periodic points,corresponding to two Lyapunov exponent values, both of which are negative (periodic attractor), (see figure 3.4*a*,3.4*b*)

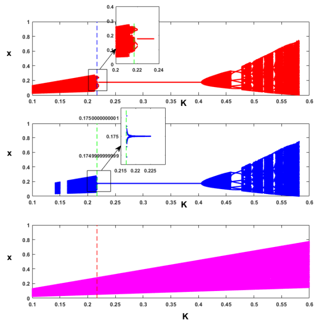

(a) Bifurcation diagram for prey population x_t with three initial conditions: $(x_1, y_1) = (0.1749, 0.5278)$: Near-equilibrium initial state $(x_2, y_2) = (0.2505, 0.1405)$: Perturbed prey-predator state $(x_3, y_3) = (0.1931, 0)$: Prey-only initial state.

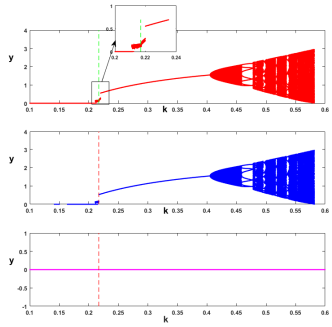

(b) Bifurcation diagram for predator population y_t with three initial conditions: $(x_1, y_1) = (0.1831, 0.9633)$: High predator density state $(x_2, y_2) = (0.1750, 1.4346)$: Extreme predator density state $(x_3, y_3) = (0.5886, 0)$: Prey-only initial state.

Figure 3.2: Bifurcation diagrams illustrating the coexistence of multiple attractors in the discrete Rosenzweig-MacArthur predator-prey model at the fixed point $P_3 = (0.175, 0.5249)$, as a function of the carrying capacity K.

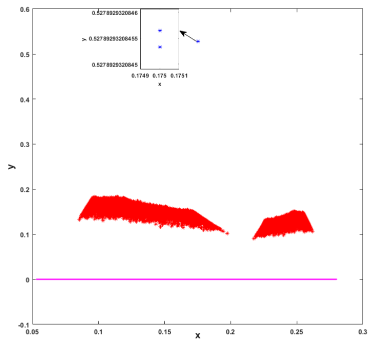

(a) Phase portrait demonstrating the coexistence of a chaotic attractor (blue) and period-2 points (red) for the parameter set (3.1). Initial conditions: $(0.2505, 0.1405)$ for the chaotic attractor and $(0.1749, 0.5278)$ for the period-2 points. The x-axis represents prey population, and the y-axis represents predator population

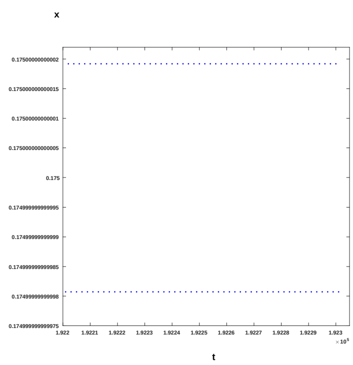

(b) Time evolution of prey population x for the periodic points, illustrating the alternating pattern characteristic of period-2 behavior. The x-axis shows time steps, and the y-axis shows prey population size.

Figure 3.3: Coexistence of multiple attractors in the discrete Rosenzweig-MacArthur predator-prey model at $P_3 = (0.175, 0.5249)$ with carrying capacity $k = 0.2171$.

4 Chaos control

This section analyzes chaos control in the Rosenzweig-MacArthur system using two approaches: the OGY method and the feedback control method, with full numerical illustrations.

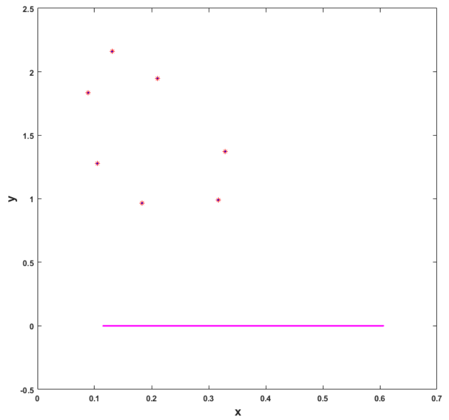

(a) Phase portrait illustrating the coexistence of a chaotic attractor (blue) and period-2 points (red) for the parameter set (3.1). Initial conditions: (0.1750, 1.4346) for the chaotic attractor and $(0.1831, 0.9633)$ for the period-7 points. The x-axis represents prey population, and the y-axis represents predator population.

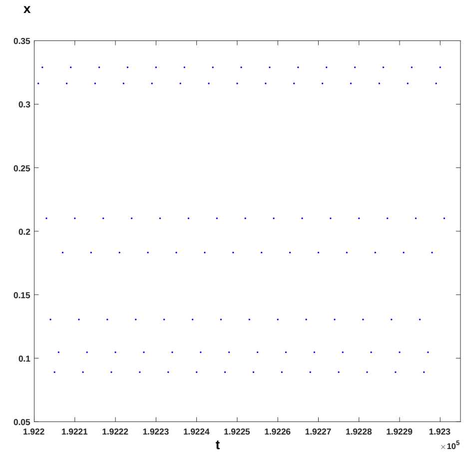

(b) Time evolution of prey population x for the periodic points, exhibiting a clear alternating pattern characteristic of period-7 behavior. The x-axis shows time steps, and the y-axis shows prey population size.

Figure 3.4: Coexistence of multiple attractors in the discrete Rosenzweig-MacArthur predator-prey model at $P_3 = (0.175, 0.5249)$ with carrying capacity $k = 0.47$.

4.1 OGY method

The OGY method stabilizes chaotic trajectories via small parameter perturbations near an unstable fixed point. Consider the discrete system together with its linearization:

$$X_{n+1} = F(X_n, p) \simeq AX_n + B, \tag{4.1}$$

where X_n is the state vector, p is the control parameter, A the Jacobian matrix, and B the control matrix. The system is controllable if the controllability matrix

$$P = [B, AB]$$

has full rank.

For the discrete model (2.3), we obtain:

$$A = \begin{pmatrix} 1 + hr - \frac{2hrx_F}{K} & -\frac{bhx_F}{x_F+H} \\ \frac{cHhy_F}{(x_F+H)^2} & 1 - hm + \frac{chx_F}{x_F+H} \end{pmatrix}, \quad B_K = \begin{pmatrix} \frac{hrx_F^2}{K^2} \\ 0 \end{pmatrix}.$$

The determinant of the controllability matrix is:

$$\det(P_K) = \frac{h^3r^3m^2H^2(K(c-m) - Hm)}{bK^*K^3(c-m)^2} \neq 0,$$

ensuring controllability when $K \neq \frac{mH}{c-m}$, $c \neq m$.

At equilibrium $P_3 = (0.1750, 0.5249)$, the Jacobian matrix is:

$$A = \begin{pmatrix} -1.1522 & -0.1800 \\ 1.6795 & 1 \end{pmatrix}, \quad B = \begin{pmatrix} 1.8243 \\ 0 \end{pmatrix}.$$

The eigenvalues are $\lambda_u = -1.0011$ and $\lambda_s = 0.8489$, confirming that P_3 is a hyperbolic saddle. The corresponding right eigenvectors are:

$$v_u = \begin{pmatrix} -0.7660 \\ 0.6429 \end{pmatrix}, \quad v_s = \begin{pmatrix} 0.0896 \\ -0.9960 \end{pmatrix},$$

and left eigenvectors:

$$f_u = \begin{pmatrix} -0.9960 \\ -0.0896 \end{pmatrix}, \quad f_s = \begin{pmatrix} -0.6429 \\ -0.7660 \end{pmatrix}.$$

Figure 4.1 illustrates that activating OGY control at $t = 100$ with a small perturbation (order 10^{-4}) in K stabilizes the system rapidly by $t = 101$.

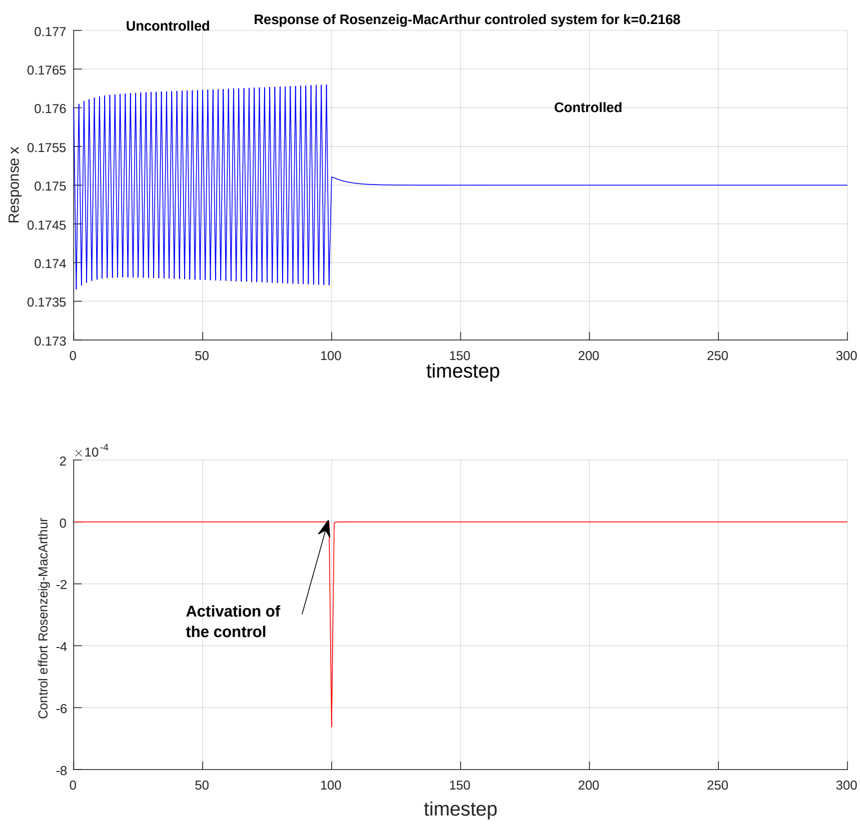

Figure 4.1: System response under OGY control with parameters (3.1), at the equilibrium $P_3 = (0.175, 0.5249)$, control gain $k = 0.2168$, and initial condition $(0.1760, 0.5259)$.

4.2 Feedback control method

In feedback control, a control force is introduced:

$$U_t = -k_1(x_t - x) - k_2(y_t - y),$$

leading to the controlled system:

$$\begin{cases} x_{t+1} = (1+hr)x_t - \frac{hr}{K}x_t^2 - \frac{hb}{x_t+H}x_t y_t - k_1(x_t - x) - k_2(y_t - y), \\ y_{t+1} = (1-hm)y_t + \frac{hc}{x_t+H}x_t y_t, \end{cases} \tag{4.2}$$

where $x = \frac{mH}{c-m}$, $y = \frac{cHr(cK-Hm-Km)}{bK(c-m)^2}$.

The Jacobian at equilibrium P_3 is:

$$J^c|_{P_3} = \begin{pmatrix} \ell_{11} - k_1 & \ell_{12} - k_2 \\ \ell_{21} & \ell_{22} \end{pmatrix},$$

where

$$\ell_{11} = 1 - \frac{hmr(c(H-K) + m(H+K))}{cK(c-m)}, \quad \ell_{12} = -\frac{bhm}{c}, \quad \ell_{21} = \frac{hr(K(c-m) - Hm)}{bK}, \quad \ell_{22} = 1.$$

The stability conditions yield the following linear equations:

$$L_1: \quad 0.5954k_1 - k_2 + 1.2814 = 0, \tag{4.3}$$

$$L_2: \quad k_2 - 0.00002545 = 0, \tag{4.4}$$

$$L_3: \quad 1.1908k_1 - k_2 + 0.0012 = 0. \tag{4.5}$$

These define a triangular stability region in the (k_1, k_2) gain parameter plane, where $|\lambda_{1,2}| < 1$ (see Figure 4.2). For $k_1 = 0.02$, $k_2 = 0.24$, the controlled system's trajectories stabilize, as shown in Figures 4.3a-4.3d.

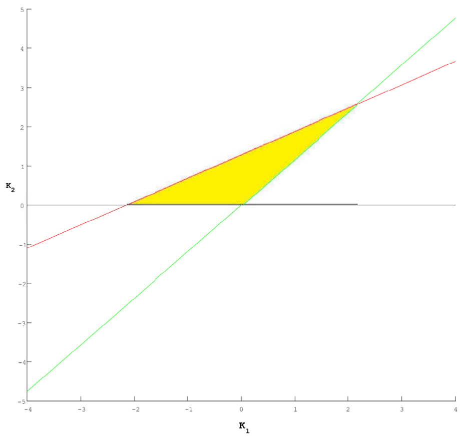

Figure 4.2: Stability region in the control gain parameters plan (k_1, k_2), for the controlled discrete Rosenzweig-MacArthur predator-prey model at the fixed point $P_3 = (0.175, 0.5249)$ for the parameter values set (3.1).

Remark 4.1. Under identical parameter settings, the OGY method stabilizes the system within approximately one time unit, while feedback control requires about 25 time units, demonstrating the superior efficiency of the OGY approach in regulating chaotic dynamics.

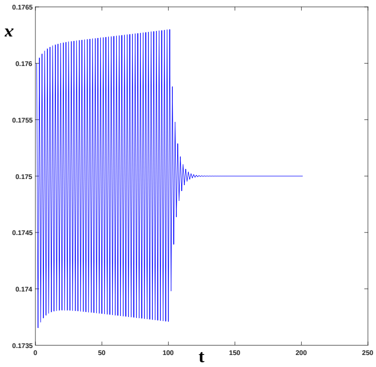

(a) Time evolution of the prey population x_t under the feedback control scheme.

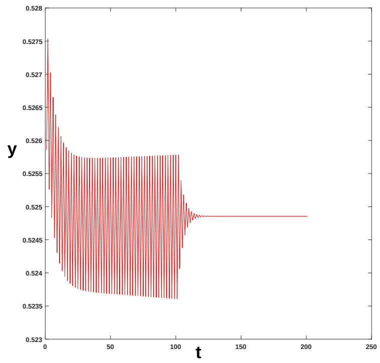

(b) Time evolution of the predator population y_t under the same feedback control parameters.

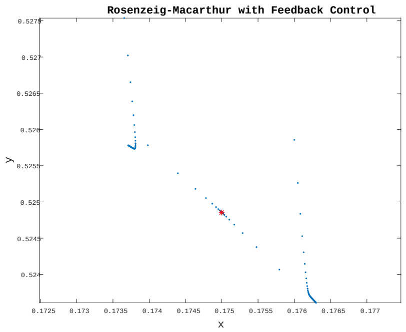

(c) Phase portrait of the controlled system (4.2) in the (x_t, y_t) plane, starting from the initial condition $(0.176, 0.5259)$. The trajectories demonstrate that the control scheme is able to stabilize the system to the fixed point $P_3 = (0.175, 0.5249)$.

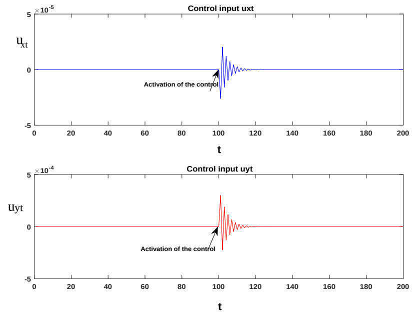

(d) Time evolution of the control inputs u_{x_t} and u_{y_t} applied to the prey and predator populations, respectively, to stabilize the system to the fixed point $P_3 = (0.175, 0.5249)$.

Figure 4.3: Stabilization of the controlled discrete Rosenzweig-MacArthur predator-prey model (4.2) at the fixed point $P_3 = (0.175, 0.5249)$ for the parameter values set (3.1) via the feedback control scheme under control gains $k_1 = 0.02$, $k_2 = 0.24$, and initial conditions $(0.176, 0.5259)$.

5 Conclusion

In this study, we identified a flip bifurcation occurring at $k = 0.2168$ within the Rosenzweig-MacArthur predator-prey model, indicating a pivotal shift in the system's dynamics.

Our findings underscore the models strong sensitivity to initial conditions, where even slight changes in starting values lead to significantly different long-term dynamics, such as convergence to a chaotic attractor, emergence of periodic cycles, or formation of invariant curves. This behavior confirms the presence of multiple coexisting attractors and the complex nature of the system.

To suppress chaotic dynamics, we explored two control approaches: the OGY method and a standard feedback control mechanism. The analysis showed that the OGY method outperformed feedback control in stabilizing the system and promoting regular dynamics.

Overall, this research contributes to a deeper understanding of nonlinear dynamics in ecological systems and illustrates the effectiveness of chaos control techniques in managing unpredictable behaviors in predator-prey interactions.

Declarations

Availability of data and materials

Not applicable.

Author's contributions

All authors contributed equally to this work. They have reviewed and approved the final manuscript.

Conflict of interest

The authors declare that they have no conflicts of interest related to this work.

Acknowledgements

The authors are grateful to the anonymous referees for their valuable suggestions and comments, which significantly improved the quality of the paper.

References

[1] M.-S. Abdelouahab and R. Lozi, *Hopf-like bifurcation and mixed mode oscillation in a fractional-order FitzHugh-Nagumo model*, *AIP Conference Proceedings* **2183**(1) (2019).

[2] M.-S. Abdelouahab and R. Lozi, *Bifurcation analysis and chaos in simplest fractional-order electrical circuit*, *Proceedings of the 3rd International Conference on Control, Engineering & Information Technology (CEIT)*, IEEE, (2015).

[3] R. Amira, M.-S. Abdelouahab, N. Touafek, M. B. Mesmouli, H. N. Zaidi and T. S. Hassan, *Nonlinear dynamic in a remanufacturing duopoly game: spectral entropy analysis and chaos control*, *AIMS Mathematics* **9**(3) (2024), 7711–7727.

[4] P. Auger, C. Lett and J. C. Poggiale, *Modélisation mathématique en écologie-2e éd.: Cours et exercices corrigés*, Dunod, Paris, (2015).

[5] M. Azioune and M.-S. Abdelouahab, *Controlling chaos and mixed mode oscillations in a Bertrand duopoly game with homogeneous expectations and quadratic cost functions*, *Mathematics and Computers in Simulation* **233** (2025), 553–566.

[6] M. Azioune, M.-S. Abdelouahab and R. Lozi, *Bifurcation Analysis of a Cournot Triopoly Game with Bounded Rationality and Chaos Control Via the OGY Method*, *International Journal of Bifurcation and Chaos* **35**(08) (2025), 2530019.

[7] S. Elaydi, *An Introduction to Difference Equations*, 3rd ed., Springer, San Antonio, (2005).

[8] A. Q. Khan, A. Maqbool and T. D. Alharbi, *Bifurcations and chaos control in a discrete Rosenzweig-Macarthur prey-predator model*, *Chaos: An Interdisciplinary Journal of Nonlinear Science* **34**(3) (2024).

[9] S. Bourafa, M.-S. Abdelouahab and R. Lozi, *On periodic solutions of fractional-order differential systems with a fixed length of sliding memory*, Journal of Innovative Applied Mathematics and Computational Sciences **1**(1) (2021), 64–78.

[10] R. Bououden, M.-S. Abdelouahab, F. Jarad and Z. Hammouch, *A novel fractional piecewise linear map: regular and chaotic dynamics*, International Journal of General Systems **50**(5) (2021), 501–526.

[11] N. Boudjerida, M.-S. Abdelouahab and R. Lozi, *Modified projective synchronization of fractional-order hyperchaotic memristor-based Chuas circuit*, Journal of Innovative Applied Mathematics and Computational Sciences **2**(3) (2022), 69–85.

[12] N. Boudjerida, M.-S. Abdelouahab and R. Lozi, *Nonlinear dynamics and hyperchaos in a modified memristor-based Chua's circuit and its generalized discrete system*, Journal of Difference Equations and Applications **29**(9-12) (2023), 1369–1390.

[13] M.K. Hassani, Y. Yazlik, N. Touafek, M.-S. Abdelouahab, M.B. Mesmouli, F.E. Mansour, *Dynamics of a higher-order three-dimensional nonlinear system of difference equations*, Mathematics, **12** (2024), 16.

[14] S. Kumar and H. Kharbanda, *Chaotic behavior of predator-prey model with group defense and non-linear harvesting in prey*, Chaos, Solitons and Fractals **119** (2019), 19–28.

[15] S. Kaouache and M.-S. Abdelouahab, *Generalized synchronization between two chaotic fractional non-commensurate order systems with different dimensions*, Nonlinear Dynamics and Systems Theory **18**(3) (2018), 273–284.

[16] Y. A. Kuznetsov, *Elements of Applied Bifurcation Theory*, 2nd ed., Springer, New York, (1998).

[17] B. Labed, S. Kaouache and M.-S. Abdelouahab, *Control of a novel class of uncertain fractional-order hyperchaotic systems with external disturbances via sliding mode controller*, Nonlinear Dynamics and Systems Theory **20**(2) (2020), 203–213.

[18] G. C. Layek, *An Introduction to Dynamical Systems and Chaos*, Springer, New Delhi, (2015).

[19] C. Lobry and T. Sari, *Migrations in the Rosenzweig-MacArthur model and the "atto-fox" problem*, Revue Africaine de Recherche en Informatique et Mathématiques Appliquées **20** (2015), 95–125.

[20] H. Meskine, M.-S. Abdelouahab and R. Lozi, *Nonlinear dynamic and chaos in a remanufacturing duopoly game with heterogeneous players and nonlinear inverse demand functions*, Journal of Difference Equations and Applications **29**(9-12) (2023), 1503–1515.

[21] W. W. Murdoch, C. J. Briggs and R. M. Nisbet, *Consumer-Resource Dynamics (MPB-36)*, Princeton University Press, (2003).

[22] K. Nadjah and M.-S. Abdelouahab, *Stability and Hopf bifurcation of the coexistence equilibrium for a differential-algebraic biological economic system with predator harvesting*, Electronic Research Archive **29**(1) (2021), 1641–1660.

[23] G. A. Polis, C. A. Myers and R. D. Holt, *The ecology and evolution of intraguild predation: potential competitors that eat each other*, *Annual Review of Ecology and Systematics* **20**(1) (1989), 297–330.

[24] H. L. Smith, *The Rosenzweig-MacArthur predator-prey model*, School of Mathematical and Statistical Sciences, (2008).

[25] Y. Wang, H. Wu and A. Wang, *A predator-prey model characterizing negative effect of prey on its predator*, *Applied Mathematics and Computation* **219**(19) (2013), 9992–9999.